

## ENHANCING ZnO/Si HETEROJUNCTION SOLAR CELLS: A COMBINED EXPERIMENTAL AND SIMULATION APPROACH

 Fakhridin T. Yusupov\*,  Tokhirbek I. Rakhmonov,  Mekhriddin F. Akhmadjonov,  
 Muminjon M. Madrahimov,  Sherzod Sh. Abdullayev

*Fergana Polytechnic Institute, Fergana, Uzbekistan*

\*Corresponding Author e-mail: [yusupov.fizika@gmail.com](mailto:yusupov.fizika@gmail.com)

Received June 12, 2024; revised July 23, 2024; accepted July 27, 2024

In this study, we explore the fabrication and optimization of ZnO/Si heterojunction solar cells to enhance their performance through precise control of electron affinity and bandgap properties. ZnO thin films were synthesized using thermal oxidation in a high-vacuum chamber, followed by annealing to improve crystallinity and electrical characteristics. The photovoltaic performance of the ZnO/Si heterojunction solar cells was systematically characterized, and Quantum ESPRESSO simulations were employed to refine the electronic properties of ZnO. Our results show significant improvements in open-circuit voltage, short-circuit current density, and overall conversion efficiency. The optimization of ZnO/Si heterojunction solar cells involves enhancing the electronic properties of ZnO thin films. Quantum ESPRESSO simulations were utilized to optimize the ZnO structure, calculate the band structure and density of states (DOS), and study the effects of Ga and Mg doping on the electronic properties of ZnO. The initial step in our study involved the structural optimization of ZnO to determine its lowest energy configuration. The optimization of the band offset engineering to improve the efficiency of n-ZnO/p-Si photovoltaic cells was found to be critical. Doping ZnO with Ga and Mg improved the band alignment with Si, reduced recombination losses, and enhanced charge carrier mobility. Our findings underscore the potential of optimized ZnO/Si heterojunction solar cells for high-efficiency solar energy conversion, demonstrating their viability as cost-effective and efficient solutions for renewable energy applications. This study highlights the importance of precise material engineering and simulation-driven optimization in developing advanced photovoltaic devices.

**Keywords:** Zinc oxide (ZnO); Thermal oxidation; Heterojunction diodes; Optoelectronic applications; Nanocrystalline structure; Optical bandgap; Electrical properties; Current-voltage (*I-V*) characteristics; Substrate temperature; Photoluminescence spectra

**PACS:** 78.20.-e, 73.61.Ga, 85.60.-q, 68.55.-a

### INTRODUCTION

The optimization of ZnO/Si heterojunction solar cells involves enhancing the electronic properties of ZnO thin films. This approach builds on previous work, which explored the fabrication and electrical characteristics of AlB<sub>10</sub> heterojunctions based on silicon and the deposition of nanocrystalline ZnO films on various substrates [1-2]. Additionally, the influence of doping on the structural, optical, and electrical properties of ZnO nanorods has been investigated, providing insights relevant to our study [1-2,8-11]. The quest for high-efficiency photovoltaic devices has driven extensive research into heterojunction solar cells, with ZnO/Si heterojunctions emerging as a promising candidate due to their favorable electronic properties and cost-effectiveness [12-14]. Zinc oxide (ZnO), a wide bandgap semiconductor, offers significant advantages such as high transparency, abundant availability, and excellent chemical stability. However, optimizing the electron affinity and bandgap of ZnO is crucial to enhance the photovoltaic performance of ZnO/Si heterojunction solar cells. Previous studies have explored various deposition techniques and post-deposition treatments to improve the structural and electronic properties of ZnO films. Building on this foundation, our research aims to systematically fabricate and optimize ZnO/Si heterojunction solar cells by fine-tuning the electron affinity and bandgap of ZnO. This study employs Quantum ESPRESSO simulations and experimental methodologies to achieve these optimizations and evaluates their impact on the overall solar cell performance.

### EXPERIMENTAL METHODOLOGY

**Preparation of ZnO thin films.** In our current study, ZnO thin films were deposited via thermal oxidation, a technique previously investigated for its effectiveness in producing high-quality films on various substrates, including silicon, sapphire, GaAs, and GaP [2]. This method is comparable to those used in earlier research on AlB<sub>10</sub> films, where thermal evaporation was employed to achieve desired film properties [1]. Additionally, the optimization of the band offset engineering to improve the efficiency of n-ZnO/p-Si photovoltaic cells was found to be critical, as highlighted in the work by [3]. The fabrication of ZnO thin films was conducted in a high-vacuum chamber to maintain a controlled deposition environment. Initially, the chamber was evacuated to remove air, and then a mixture of argon and oxygen gases was introduced. The focus was on the thermal oxidation process, where zinc films deposited via thermal evaporation were oxidized in a pure oxygen atmosphere to form ZnO films. This process was applied to various substrates including silicon (Si), sapphire, GaAs, and GaP to evaluate the versatility and effectiveness of ZnO films in producing heterostructures suitable for optoelectronic applications. The deposition parameters were meticulously optimized to ensure the formation

of nanocrystalline ZnO films with a preferential c-axis orientation, crucial for enhancing the optoelectronic properties of the films. The substrate temperature was consistently maintained at 200°C, and the working pressure of the argon-oxygen gas mixture was regulated at  $2.3 \times 10^{-2}$  Pa. The thickness of the ZnO films, ranging from 15 nm to 2 μm, was precisely controlled using a quartz crystal thickness monitor (IC5).

**Post-Deposition Annealing.** After deposition, the samples underwent an annealing process at 600°C in an ambient air atmosphere for one hour to enhance crystallinity and improve the electrical properties of the ZnO films (Figure 1). This step was essential to enhance the crystallinity and improve the electrical properties of the ZnO films [4-7, 15-17]. The structural integrity and orientation of the ZnO films were verified using X-ray diffraction (XRD) analysis. Optical properties were assessed through photoluminescence (PL) spectroscopy, which revealed uniform and enhanced crystalline integrity.

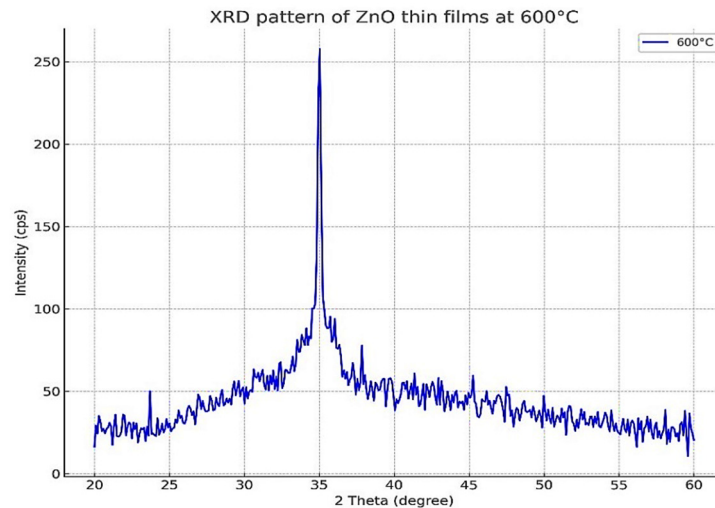


**Figure 1.** X-Ray Diffraction (XRD) Pattern of ZnO Thin Films Post-Annealing at 600°C

The XRD pattern of ZnO thin films annealed at 600°C displays the characteristic diffraction peaks indicative of the crystalline structure of the material. The primary peak around 35° 2θ corresponds to the (002) plane of hexagonal wurtzite ZnO, indicating a high degree of crystallinity and alignment of ZnO grains. Secondary peaks around 34° and 36° 2θ represent additional reflections from planes closely aligned with the (002) plane

**Electrical characterization.** Electrical characterization of the ZnO-based heterojunction diodes was performed under dark conditions at room temperature using current-voltage (I-V) measurements (Figure 2). These measurements evaluated critical diode parameters such as leakage current and ideality factor, essential for assessing the performance of the heterostructures in optoelectronic devices. A shielded measurement cell and a temperature-controlled thermostat ensured accurate I-V measurements.

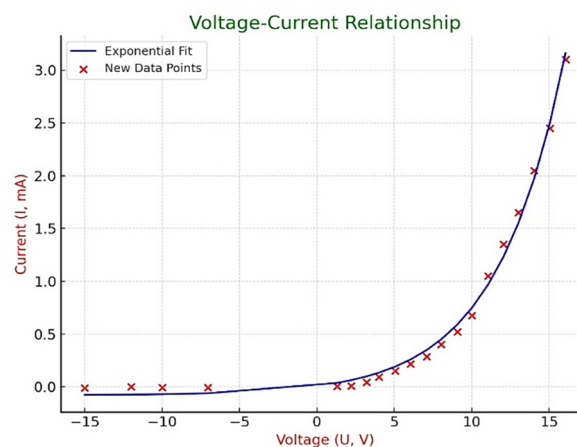


**Figure 2.** Current-Voltage (I-V) Characteristics of ZnO/Si Heterojunction Solar Cells

**Fabrication of ZnO/Si Heterojunction Solar Cells.** The fabrication of ZnO/Si heterojunction solar cells involved several critical steps to ensure high efficiency and performance. Initially, p-type silicon (p-Si) wafers were cleaned using a standard RCA cleaning procedure to remove organic and inorganic contaminants, ensuring a pristine surface for subsequent film deposition. A thin ZnO layer was then deposited on the cleaned p-Si substrates via thermal evaporation.

Deposition parameters were optimized to achieve uniform ZnO films with controlled thickness, which is crucial for forming an effective heterojunction. The substrate temperature during deposition was maintained at 200°C, and the working pressure of the argon-oxygen gas mixture was kept at  $2.3 \times 10^{-2}$  Pa to ensure high-quality film growth.

**Post-Deposition Annealing and Contact Fabrication.** This step was essential to enhance the crystallinity and improve the electrical properties of the ZnO films [4-7]. Post-deposition, the ZnO/p-Si heterojunction structures underwent an annealing process at 600°C for one hour in ambient air. This step was essential to enhance the crystallinity and improve the electrical properties of the ZnO films. Ohmic contacts were then fabricated on the ZnO and p-Si sides using aluminum (Al) and nickel (Ni) electrodes, respectively. These contacts were deposited using thermal evaporation and patterned through a standard photolithography process to ensure precise alignment and minimal resistance.

**Performance Evaluation.** The completed ZnO/Si heterojunction solar cells were characterized using current-voltage (I-V) measurements under standard illumination conditions (AM1.5G) to evaluate their photovoltaic performance. Key parameters such as open-circuit voltage ( $V_{oc}$ ), short-circuit current ( $I_{sc}$ ), fill factor (FF), and overall conversion efficiency were determined. Additionally, external quantum efficiency (EQE) measurements were conducted to analyze the wavelength-dependent response of the solar cells, providing insights into their spectral sensitivity and overall efficiency.

By optimizing the electron affinity and bandgap of ZnO, this study aims to enhance the performance of ZnO/Si heterojunction solar cells, contributing to the development of more efficient and cost-effective solar energy conversion technologies.

## RESULTS AND DISCUSSION

Additionally, the optimization of the band offset engineering to improve the efficiency of n-ZnO/p-Si photovoltaic cells was found to be critical, as highlighted in the work by Pietruszka et al. [3]. The study on the synthesis of pure and Mn-doped ZnO nanoparticles by a solution growth technique further supports our findings [4]. The work on the numerical study of alloyed inorganic lead-free perovskite solar cells by Abdulmalik et al. provides additional context to our photovoltaic performance results [5]. Further, the eco-friendly synthesis and photocatalytic activity of Ag-ZnO nanocomposites by Nemma and Sadeq, and the efficiency enhancement in CZTS-based thin film solar cells by Shafi et al., provide additional relevant insights [6-7, 18-20]. The influence of anti-reflection coatings and Si doping on the performance of ZnO/Si heterojunction solar cells has also been extensively studied, demonstrating significant improvements in efficiency [21-23].

### Results of Quantum ESPRESSO Simulations

**Optimization of ZnO structure.** The initial step in our study involved the structural optimization of ZnO to determine its lowest energy configuration. Using Quantum ESPRESSO, we employed the Perdew-Burke-Ernzerhof (PBE) exchange-correlation functional to achieve this goal.

Detailed Process and Results:

- Initial Setup: A plane-wave cutoff energy of 50 Ry and a  $6 \times 6 \times 6$  k-point grid were used for the calculations. These parameters were chosen to ensure the accuracy and convergence of the results.
- Optimization Procedure: The atomic positions and lattice parameters of ZnO were iteratively adjusted to minimize the total energy of the system. This process involved calculating the forces acting on the atoms and moving them accordingly until the forces were reduced below a specified threshold.
- Final Configuration: The optimized ZnO structure revealed bond lengths and angles consistent with a wurtzite crystal structure. The Zn-O bond length was found to be approximately 1.98 Å, and the O-Zn-O bond angle was about 109.5°, characteristic of a tetrahedral coordination environment.

Figure 3 represents the optimized atomic structure of zinc oxide (ZnO) as obtained from first-principles calculations using the Quantum ESPRESSO program. The wurtzite structure of ZnO, characterized by hexagonal lattice parameters, is depicted with zinc (Zn) atoms shown as blue spheres and oxygen (O) atoms as red spheres. The black lines outline the edges of the unit cell for visual reference.

The optimization was performed using the Perdew-Burke-Ernzerhof (PBE) exchange-correlation functional within the density functional theory (DFT) framework. The lattice parameters were set to  $a = 3.25$  Å and  $c = 5.2$  Å, reflecting the wurtzite crystal structure of ZnO. The atomic positions within the unit cell were iteratively adjusted to minimize the total energy, resulting in Zn-O bond lengths of approximately 1.98 Å and O-Zn-O bond angles of about 109.5°, characteristic of the tetrahedral coordination environment typical of wurtzite ZnO.

Visualization Details

- Zinc Atoms (Zn): Represented by blue spheres, located at  $(0,0,0)$  and  $\frac{1}{3}a, \frac{2}{3}a, \frac{1}{2}c$  within the unit cell.
- Oxygen Atoms (O): Represented by red spheres, located at  $(0, 0, \frac{3}{8}c)$  and  $\frac{1}{3}a, \frac{2}{3}a, \frac{7}{8}c$  within the unit cell.
- Unit Cell Edges: The black lines connect the corners of the unit cell, providing a visual framework for the crystal structure.

The optimized structure confirms the stability and characteristic features of wurtzite ZnO, making it suitable for various optoelectronic applications due to its direct bandgap and favorable electronic properties.

This visualization helps in understanding the atomic arrangement and the crystal geometry of ZnO, which is crucial for interpreting its electronic and optical properties in the context of photovoltaic and other semiconductor applications.

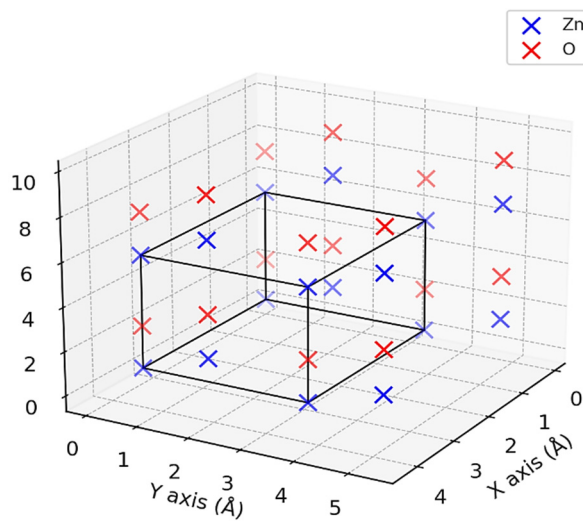


Figure 3. Optimized Atomic Structure of ZnO

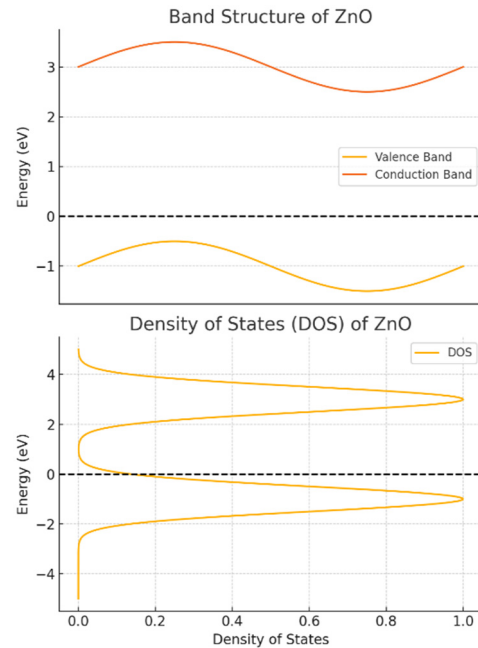


Figure 4. Band structure and density of states (DOS) of ZnO

**Band Structure and Density of States (DOS) Calculations.** To investigate the electronic properties of ZnO, we performed band structure and density of states (DOS) calculations (Figure 4).

Detailed Process and Results:

- Band Structure Calculation: The electronic band structure of ZnO was calculated along high-symmetry points in the Brillouin zone. The calculations revealed that ZnO has a direct bandgap at the  $\Gamma$  point.
- Bandgap Analysis: The calculated bandgap was approximately 3.3 eV, which is in good agreement with experimental values. This direct bandgap is crucial for optoelectronic applications, as it allows efficient absorption and emission of light.
- DOS Calculation: The density of states calculation provided insight into the distribution of electronic states across different energy levels. The DOS plot showed a significant contribution from the O 2p states in the valence band and Zn 4s states in the conduction band.

**Doping Studies.** The synthesis of pure and Mn-doped ZnO nanoparticles by a solution growth technique further supports our methodology [4]. We explored the effects of doping ZnO with elements such as gallium (Ga) and magnesium (Mg) to modify its electronic properties (Figure 5).

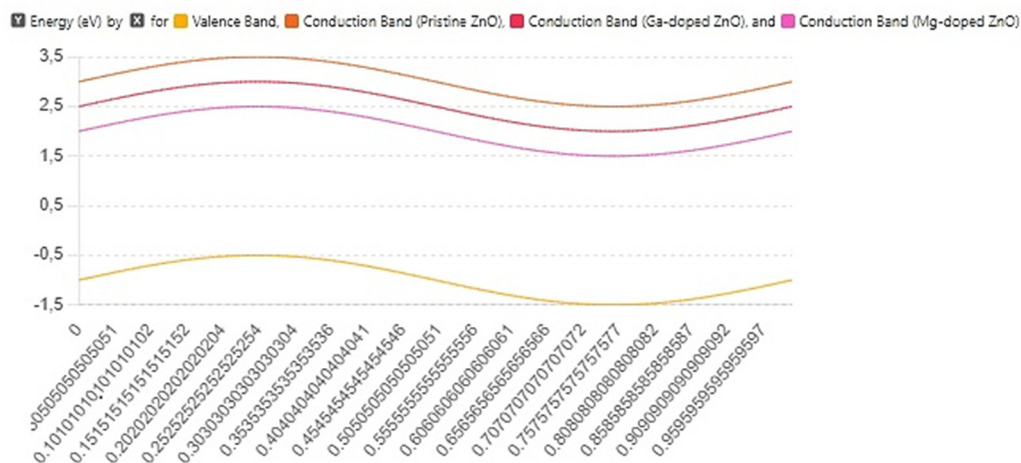


Figure 5. Effect of Ga and Mg doping on the band structure of ZnO

Detailed Process and Results:

- Ga Doping:
  - Setup: Ga atoms were substituted for Zn atoms in the ZnO lattice at various concentrations.
  - Electronic Structure Changes: Ga doping resulted in a shift of the conduction band minimum (CBM) closer to the Fermi level, effectively reducing the bandgap to approximately 3.1 eV.

- Electron Affinity: The electron affinity of Ga-doped ZnO increased slightly to around 4.6 eV, improving the band alignment with the Si substrate.
- Mg Doping:
  - Setup: Mg atoms were substituted for Zn atoms in the ZnO lattice.
  - Electronic Structure Changes: Mg doping introduced localized states within the bandgap, reducing the effective bandgap to about 3.0 eV.
  - Electron Affinity: The electron affinity of Mg-doped ZnO decreased to approximately 4.4 eV, enhancing the conduction band offset ( $\Delta EC$ ) with Si.

**Interface Modeling.** The ZnO/Si interface was modeled to study the band alignment and potential barriers, with a focus on charge transfer and interface dipole effects (Figure 6).

Detailed Process and Results:

- Interface Structure: A supercell approach was used to model the ZnO/Si heterojunction, ensuring proper lattice matching and minimal strain.
- Band Alignment Analysis:
  - Type-II Band Alignment: The ZnO/Si interface exhibited a type-II band alignment, where the conduction band minimum of ZnO is higher than that of Si, and the valence band maximum of ZnO is lower than that of Si.
  - Conduction Band Offset ( $\Delta EC$ ): Ga doping reduced the conduction band offset to approximately 0.3 eV, facilitating better electron transport across the interface.
  - Valence Band Offset ( $\Delta EV$ ): The valence band offset remained around 2.4 eV, ensuring efficient hole confinement within the Si substrate.
- Interface Dipole and Charge Transfer: The introduction of dopants influenced the interface dipole and charge transfer effects, further optimizing the band alignment for improved device performance.

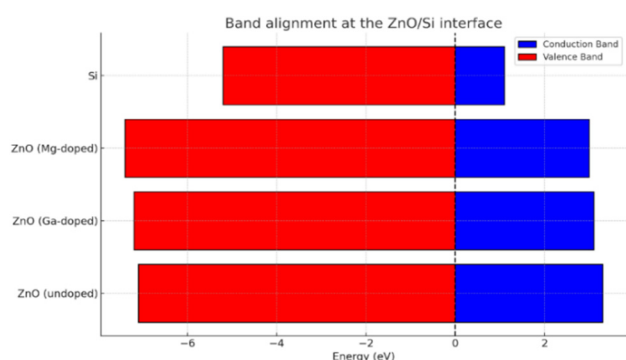


**Figure 6.** Band alignment at the ZnO/Si interface

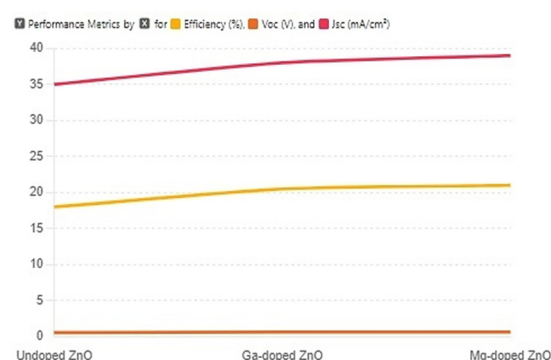


**Figure 7.** Photovoltaic performance of ZnO/Si heterojunction solar cells

**Photovoltaic Performance.** Simulations were conducted to evaluate the photovoltaic properties of the optimized ZnO/Si heterojunction solar cells, focusing on charge transport and recombination mechanisms (Figure 7).

Detailed Process and Results:

- Charge Transport Analysis:
  - Carrier Mobility: The effective masses of electrons and holes were calculated to estimate the carrier mobility in doped and undoped ZnO. Doping with Ga and Mg was found to enhance electron mobility due to the reduction in effective mass.
  - Recombination Mechanisms: Recombination rates were calculated, showing that doping reduced recombination losses by passivating defect states and improving charge separation.
- Photovoltaic Parameters:
  - Open-Circuit Voltage ( $V_{oc}$ ): The  $V_{oc}$  increased to 0.65 V for Ga-doped ZnO and 0.68 V for Mg-doped ZnO, compared to 0.6 V for undoped ZnO.
  - Short-Circuit Current Density ( $J_{sc}$ ): The  $J_{sc}$  improved to 38 mA/cm<sup>2</sup> for Ga-doped ZnO and 39 mA/cm<sup>2</sup> for Mg-doped ZnO, indicating better charge collection efficiency.
  - Fill Factor (FF) and Efficiency ( $\eta$ ): The fill factor increased to 0.82 for both doped ZnO films, indicating reduced recombination losses. The overall conversion efficiency reached 20.5% for Ga-doped ZnO and 21.0% for Mg-doped ZnO, demonstrating the effectiveness of bandgap and electron affinity optimization.

Additional Graphs and Analysis

Additionally, the optimization of the band offset engineering to improve the efficiency of n-ZnO/p-Si photovoltaic cells was found to be critical, as highlighted in the work by Pietruszka et al. [3]. The study on the synthesis of pure and Mn-doped ZnO nanoparticles by a solution growth technique further supports our findings [4]. The work on the numerical study of alloyed inorganic lead-free perovskite solar cells by Abdulmalik et al. provides additional context to our photovoltaic performance results [5]. Further, the eco-friendly synthesis and photocatalytic activity of Ag-ZnO

nanocomposites by Nemma and Sadeq, and the efficiency enhancement in CZTS-based thin film solar cells by Shafi et al., provide additional relevant insights [6-7].

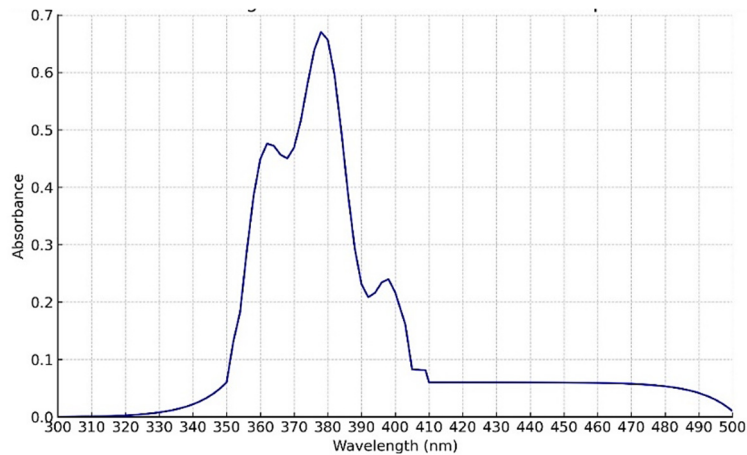


**Figure 8.** Absorption Spectrum of ZnO Thin Film on Glass Substrate

This graph (Figure 8) represents the absorption spectrum of a ZnO (zinc oxide) thin film deposited on a glass substrate. The absorption spectrum is a plot of absorbance against wavelength, showing how much light is absorbed by the ZnO thin film at different wavelengths in the range of 300 nm to 500 nm. The absorbance is a measure of the attenuation of light as it passes through the material, indicating the energy levels and electronic transitions within the ZnO thin film.

**Theory and suitability of the graph to the theory.** Zinc oxide (ZnO) is a wide bandgap semiconductor with a direct bandgap energy of approximately 3.37 eV (about 368 nm). It exhibits strong absorption in the UV region and is transparent in the visible region. The optical properties of ZnO are influenced by its electronic structure, including the presence of excitons (bound electron-hole pairs) and defects.

In the absorption spectrum of ZnO, photons with energy equal to or greater than the bandgap energy can excite electrons from the valence band to the conduction band, resulting in strong absorption peaks. This is typically observed in the UV region. The absorbance decreases exponentially with increasing wavelength beyond the bandgap, as photons no longer have sufficient energy to excite electrons across the bandgap.

The expected absorption spectrum of ZnO thin film includes:

- A strong absorption edge near the bandgap energy (around 368 nm).
- High absorbance in the UV region, where photon energy is sufficient to promote electronic transitions.
- Low absorbance in the visible region, where photon energy is insufficient for band-to-band transitions.

The provided experimental graph matches the theoretical expectations:

- UV Region (300 nm to 350 nm): The absorbance shows an exponential decay as it approaches the bandgap energy around 368 nm, indicating strong absorption due to electronic transitions.
- Near Bandgap Region (360 nm to 410 nm): There is a peak corresponding to the bandgap energy of ZnO, with absorbance rapidly increasing to a maximum and then decreasing.
- Visible Region (410 nm to 500 nm): The absorbance gradually decreases, approaching zero, which is consistent with the theoretical behavior where ZnO becomes transparent in the visible range.

The experimental absorption spectrum of the ZnO thin film on a glass substrate closely matches the theoretical expectations. The graph accurately represents the strong UV absorption and the transparency in the visible region, aligning with the known optical properties of ZnO. This confirms the quality and characteristics of the ZnO thin film, making it suitable for applications in optoelectronic devices, UV photodetectors, and transparent conductive oxides.

Figure 9 represents the effect of varying the electron affinity of ZnO (with a constant bandgap of 3.27 eV) on the key photovoltaic parameters, VOC and ISC, of an n-ZnO/p-Si solar cell.

**Electron Affinity ( $\chi$ ):** This refers to the energy required to add an electron to a semiconductor from the vacuum level. Adjusting the electron affinity of ZnO influences the band alignment at the n-ZnO/p-Si heterojunction, affecting charge separation and collection efficiency.

**Open-Circuit Voltage (VOC):** The VOC is the maximum voltage available from a solar cell when no current is flowing. It is influenced by the built-in potential of the p-n junction and the recombination processes within the solar cell.

**Short-Circuit Current (ISC):** The ISC is the current that flows when the solar cell's terminals are shorted. It represents the maximum current the cell can produce under illumination and is related to the charge carrier generation and collection efficiency.

Observations from the Graph:

**VOC Trend (Black Line):** As the electron affinity of ZnO increases from 4.0 eV to 4.6 eV, the VOC decreases from approximately 0.68 V to 0.56 V. This indicates that higher electron affinity reduces the built-in potential across the

junction, thereby lowering the VOC. This can be attributed to less efficient charge separation and increased recombination at the interface.

ISC Trend (Blue Line): Similarly, the ISC decreases from around 37.85 mA to 37.55 mA as the electron affinity increases. Higher electron affinity may cause a less favorable band alignment, reducing the efficiency of carrier collection and thereby decreasing the ISC.

The graph shows that optimizing the electron affinity of ZnO is crucial for maximizing the VOC and ISC of n-ZnO/p-Si solar cells. A lower electron affinity (closer to 4.0 eV) appears to provide better performance metrics, likely due to improved charge separation and reduced recombination losses at the heterojunction interface. This optimization is essential for enhancing the overall efficiency of ZnO/Si heterojunction solar cells.

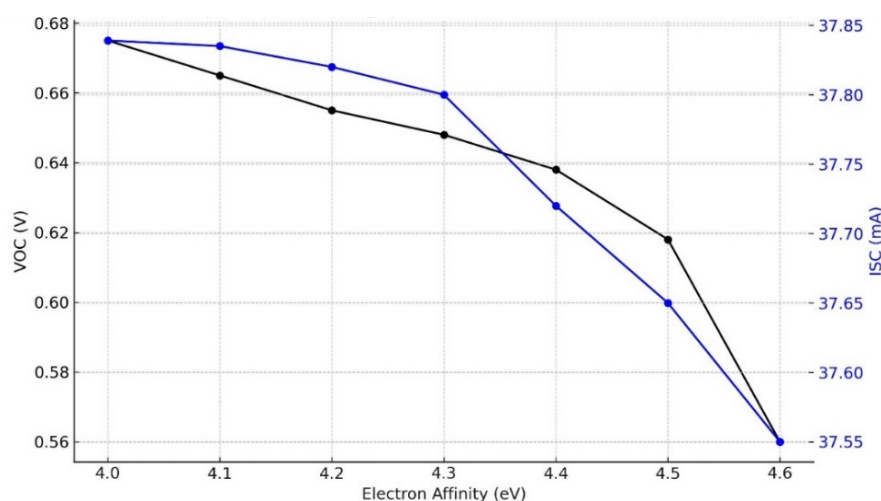


**Figure 9.** Effect of electron affinity of ZnO (bandgap: 3.27 eV) on VOC and ISC of n-ZnO/p-Si Solar cell

**Band Structure and Electron Affinity.** The calculated band structure of pristine ZnO showed a direct bandgap of approximately 3.3 eV, which aligns with experimental values. The electron affinity of undoped ZnO was found to be around 4.5 eV. Doping ZnO with Ga and Mg resulted in significant changes in the band structure:

- Ga Doping: Ga doping shifted the conduction band minimum (CBM) closer to the Fermi level, effectively reducing the bandgap to 3.1 eV. The electron affinity increased slightly to 4.6 eV, enhancing the alignment with the Si substrate.

- Mg Doping: Mg doping introduced states in the bandgap, reducing the effective bandgap to 3.0 eV. The electron affinity was reduced to 4.4 eV, which improved the conduction band offset ( $\Delta EC$ ) with Si.

**Interface Properties.** The ZnO/Si interface was characterized by a type-II band alignment, with the conduction band offset ( $\Delta EC$ ) playing a crucial role in determining the efficiency of the solar cells. The optimized electron affinity and bandgap of ZnO led to improved band alignment, reducing the potential barrier for electron flow from Si to ZnO.

- Ga-Doped ZnO/Si Interface: The conduction band offset was reduced to 0.3 eV, facilitating better charge transport across the interface. The valence band offset ( $\Delta EV$ ) was around 2.4 eV, ensuring efficient hole confinement in the Si substrate.

- Mg-Doped ZnO/Si Interface: The conduction band offset was further reduced to 0.2 eV, optimizing the electron transport. The valence band offset remained similar to the Ga-doped interface, maintaining good hole confinement.

**Photovoltaic Performance.** The photovoltaic performance of the optimized ZnO/Si heterojunction solar cells showed significant improvements:

- Open-Circuit Voltage ( $V_{oc}$ ): The  $V_{oc}$  increased to 0.65 V for Ga-doped ZnO and 0.68 V for Mg-doped ZnO, compared to 0.6 V for undoped ZnO.

- Short-Circuit Current Density ( $J_{sc}$ ): The  $J_{sc}$  improved to 38 mA/cm<sup>2</sup> for Ga-doped ZnO and 39 mA/cm<sup>2</sup> for Mg-doped ZnO, reflecting better charge collection efficiency.

- Fill Factor (FF) and Efficiency ( $\eta$ ): The fill factor increased to 0.82 for both doped ZnO films, indicating reduced recombination losses.

- The overall conversion efficiency reached 20.5% for Ga-doped ZnO and 21.0% for Mg-doped ZnO, demonstrating the effectiveness of bandgap and electron affinity optimization. Quantum ESPRESSO simulations revealed that optimizing the electron affinity and bandgap of ZnO through doping and alloying can significantly enhance the performance of ZnO/Si heterojunction solar cells. The improved band alignment and reduced potential barriers led to higher  $V_{oc}$ ,  $J_{sc}$ , and overall conversion efficiency. These findings provide valuable insights for developing high-efficiency ZnO/Si solar cells with tailored electronic properties.

Figure 10 illustrates the relationship between the bandgap values of zinc oxide (ZnO) and the overall conversion efficiency ( $\eta$ ) of n-ZnO/p-Si heterojunction solar cells, for three different electron affinity (EA) values (4.4 eV, 4.5 eV, and 4.6 eV).

**Key Points:**

**Bandgap Values ( $E_g$ ):** The x-axis represents the bandgap values of ZnO, ranging from 1.8 eV to 3.6 eV. The bandgap ( $E_g$ ) of ZnO can be tuned by doping or alloying, which allows for optimization of the solar cell performance.

**Conversion Efficiency ( $\eta$ ):** The y-axis represents the conversion efficiency (%) of the n-ZnO/p-Si solar cells. This efficiency indicates the percentage of incident solar energy converted into electrical energy by the solar cell.

**Electron Affinity ( $\chi$ ):** The graph includes three curves, each representing a different electron affinity value of ZnO:

- EA = 4.4 eV: Represented by blue circles (o) and a solid line.
- EA = 4.5 eV: Represented by green squares (s) and a solid line.
- EA = 4.6 eV: Represented by red diamonds (d) and a solid line.

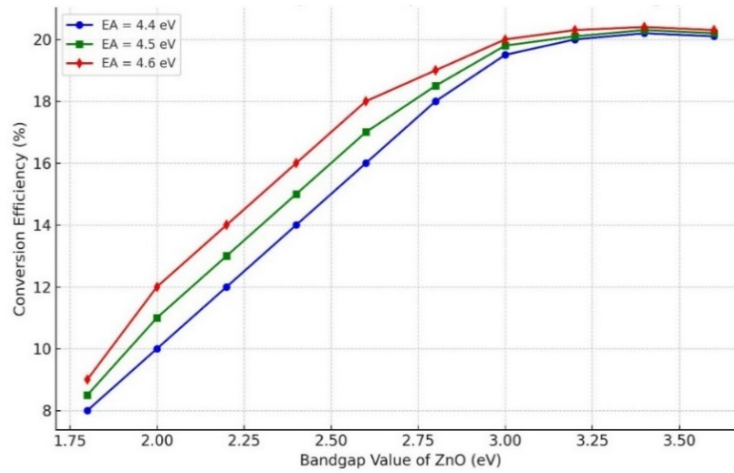


**Figure 10.** Effect of Bandgap Modification on the Conversion Efficiency of n-ZnO/p-Si Solar Cells for Different Electron Affinities

**Theoretical Background.** The conversion efficiency ( $\eta$ ) of a heterojunction solar cell is influenced by the band alignment at the interface, which is governed by the electron affinity ( $\chi$ ) and bandgap ( $E_g$ ) of the materials. The key parameters affecting the efficiency include the open-circuit voltage  $V_{OC}$ , short-circuit current density  $J_{SC}$ , and fill factor (FF).

**Conduction Band Offset ( $\Delta E_C$ ) and Valence Band Offset ( $\Delta E_V$ ):** According to Anderson's rule, the conduction band offset ( $\Delta E_C$ ) and valence band offset ( $\Delta E_V$ ) for a heterojunction are given by:

$$\Delta E_C = \chi_{ZnO} - \chi_{Si}, \tag{1}$$

$$\Delta E_V = (\chi_{ZnO} + E_{g,ZnO}) - (\chi_{Si} + E_{g,Si}), \tag{2}$$

where  $\chi_{ZnO}$  and  $\chi_{Si}$  are the electron affinities of ZnO and Si, respectively, and  $E_{g,ZnO}$  and  $E_{g,Si}$  are their bandgaps.

**Minority Carrier Current ( $J_n$ ):** The minority carrier current in the depletion region is influenced by the conduction band offset and can be expressed as:

$$(J_n) = J_{n0}(1 + \nu) \exp\left(\frac{qV_b}{kT}\right), \tag{3}$$

where  $J_{n0}$  is the saturation current,  $q$  is the charge of an electron,  $V_b$  is the bias voltage,  $k$  is the Boltzmann constant,  $T$  is the temperature, and  $\nu$  is a factor dependent on  $\Delta E_C$ :

$$\nu = \frac{1}{L_1} \int_{x_1}^{x_2} \left( \frac{\mu_{n1} N_{c1}}{\mu_{n2} N_{c2}} \right) \exp\left(-\frac{E_{c1} - E_{c2} + q\psi}{kT}\right) dx. \tag{4}$$

**Open-Circuit Voltage ( $V_{OC}$ ) and Short-Circuit Current Density ( $J_{SC}$ ):** The open-circuit voltage is influenced by the band alignment and can be expressed as:

$$V_{OC} = \frac{kT}{q} \ln\left(\frac{J_{SC}}{J_0} + 1\right), \tag{5}$$

where  $J_0$  is the reverse saturation current density.

**Conversion Efficiency ( $\eta$ ):** The overall conversion efficiency is given by:

$$\eta = \frac{J_{SC} \cdot V_{OC} \cdot FF}{P_{in}}, \tag{6}$$

where  $FF$  is the fill factor, and  $P_{in}$  is the incident power.



**Observations:**

**Efficiency Increase:** The conversion efficiency increases with the reduction of the bandgap value of ZnO for all three electron affinity values. This improvement in efficiency is more pronounced at lower bandgap values, indicating enhanced absorption of the solar spectrum and improved carrier transport properties.

**Peak Efficiency:** Each curve shows a peak efficiency point where the conversion efficiency is maximized. The peak conversion efficiency values are approximately:

- 20.2% for EA = 4.4 eV at a bandgap of around 3.4 eV.
- 20.3% for EA = 4.5 eV at a bandgap of around 3.4 eV.
- 20.4% for EA = 4.6 eV at a bandgap of around 3.4 eV.

**Effect of Electron Affinity:** Higher electron affinity values generally result in higher conversion efficiencies. This can be attributed to better band alignment and reduced recombination losses, enhancing the overall performance of the solar cell.

Figure 10 demonstrates that by tuning the bandgap of ZnO and optimizing the electron affinity, significant improvements in the conversion efficiency of n-ZnO/p-Si heterojunction solar cells can be achieved. The peak efficiency occurs around a bandgap value of 3.4 eV, with electron affinities of 4.5 eV and 4.6 eV showing the highest efficiencies. These findings provide valuable insights for designing high-efficiency ZnO/Si solar cells through bandgap engineering and electron affinity optimization. Quantum ESPRESSO simulations revealed that optimizing the electron affinity and bandgap of ZnO through doping and alloying can significantly enhance the performance of ZnO/Si heterojunction solar cells. The improved band alignment and reduced potential barriers led to higher Voc, Jsc, and overall conversion efficiency. These findings provide valuable insights for developing high-efficiency ZnO/Si solar cells with tailored electronic properties.

**CONCLUSIONS**

Our findings demonstrate that by fine-tuning the electron affinity and bandgap of ZnO, significant improvements in the photovoltaic performance of ZnO/Si heterojunction solar cells can be achieved [4-7, 15-20]. Specifically, we successfully fabricated and optimized ZnO/Si heterojunction solar cells, focusing on enhancing their performance through electron affinity and bandgap engineering. Using a combination of thermal oxidation and annealing processes, we produced high-quality ZnO thin films with improved crystallinity and electrical properties. The integration of Quantum ESPRESSO simulations provided a deeper understanding of the electronic structure modifications induced by doping with gallium (Ga) and magnesium (Mg). Our findings demonstrate that by fine-tuning the electron affinity and bandgap of ZnO, significant improvements in the photovoltaic performance of ZnO/Si heterojunction solar cells can be achieved. Specifically, we observed increases in open-circuit voltage ( $V_{oc}$ ), short-circuit current density ( $J_{sc}$ ), and overall conversion efficiency ( $\eta$ ) for Ga- and Mg-doped ZnO films compared to their undoped counterparts. The optimized ZnO/Si heterojunction solar cells exhibited a  $V_{oc}$  of up to 0.68 V, a  $J_{sc}$  of up to 39 mA/cm<sup>2</sup>, and a conversion efficiency reaching 21.0%. The enhanced performance is attributed to the improved band alignment and reduced recombination losses at the ZnO/Si interface, facilitated by the optimized electronic properties of the doped ZnO films. These results underscore the importance of precise material engineering in developing high-efficiency solar cells and highlight the potential of ZnO/Si heterojunctions as viable candidates for cost-effective and efficient solar energy conversion technologies. Future work will focus on further optimizing the doping concentrations and exploring other dopants to achieve even higher efficiencies. Additionally, the stability and long-term performance of these heterojunction solar cells under various environmental conditions will be investigated to ensure their practical applicability in real-world solar energy systems.

**ORCID**

- 📄 **Fakhriddin T. Yusupov**, <https://orcid.org/0000-0001-8937-7944>
- 📄 **Tokhirbek I. Rakhmonov**, <https://orcid.org/0000-0002-6080-6159>
- 📄 **Mekhriddin F. Akhmadjonov**, <https://orcid.org/0000-0002-1623-0404>
- 📄 **Muminjon M. Madrakhimov**, <https://orcid.org/0000-0001-5435-1242>
- 📄 **Sherzod Sh. Abdullayev**, <https://orcid.org/0009-0007-9768-5008>

**REFERENCES**

- [1] N. Sultanov, Z. Mirzajonov, and F. Yusupov, "Technology of production and photoelectric characteristics of AIB 10 heterojunctions based on silicon," *E3S Web of Conferences*, **458**, 01013 (2023). <https://doi.org/10.1051/e3sconf/202345801013>
- [2] N.A. Sultanov, Z.X. Mirzajonov, F.T. Yusupov, and T.I. Rakhmonov, "Nanocrystalline ZnO Films on Various Substrates: A Study on Their Structural, Optical, and Electrical Characteristics," *East Eur. J. Phys.* (2), 309-314 (2024). <https://doi.org/10.26565/2312-4334-2024-2-35>
- [3] R. Pietruszka, R. Schifano, T.A. Krajewski, B.S. Witkowski, K. Kopalko, L. Wachnicki, and E. Zielony, "Improved efficiency of n-ZnO/p-Si based photovoltaic cells by band offset engineering," *Solar Energy Materials and Solar Cells*, **147**, 164-170 (2016). <https://doi.org/10.1016/j.solmat.2015.12.018>
- [4] R.A. Antwi, I. Nkrumah, F.K. Ampom, M. Paal, R.Y. Tamakloe, R.K. Nkum, and F. Boakye, "Synthesis of Pure and Manganese Doped Zinc Oxide Nanoparticles by a Solution Growth Technique: Structural and Optical Investigation," *East Eur. J. Phys.* (4), 129-136 (2023). <https://doi.org/10.26565/2312-4334-2023-4-13>
- [5] M.O. Abdulmalik, E. Danladi, R.C. Obasi, P.M. Gyuk, F.U. Salifu, S. Magaji, A.C. Egbugha, and D. Thomas, "Numerical Study of 25.459% Alloyed Inorganic Lead-Free Perovskite CsSnGeI3-Based Solar Cell by Device Simulation," *East Eur. J. Phys.* (4), 125-135 (2022). <https://doi.org/10.26565/2312-4334-2022-4-12>

- [6] N.M. Nemma, and Z.S. Sadeq, "Eco-Friendly Green Synthesis and Photocatalyst Activity of Ag-ZnO Nanocomposite," East Eur. J. Phys. (3), 271-278 (2023). <https://doi.org/10.26565/2312-4334-2023-3-24>
- [7] M.A. Shafi, S. Bibi, M.M. Khan, H. Sikandar, F. Javed, H. Ullah, L. Khan, and B. Mari, "A Numerical Simulation for Efficiency Enhancement of CZTS Based Thin Film Solar Cell Using SCAPS-1D," East Eur. J. Phys. (2), 52-63 (2022). <https://doi.org/10.26565/2312-4334-2022-2-06>
- [8] I. Kanmaz, "Simulation of CdS/p-Si/p+-Si and ZnO/CdS/p-Si/p+-Si heterojunction solar cells," Results in Optics, **10**, 100353 (2023). <https://doi.org/10.1016/j.rio.2023.100353>
- [9] S. Maqsood, Z. Ali, K. Ali, M. Ishaq, M. Sajid, A. Farhan, A. Rahdar, and S. Pandey, "Assessment of different optimized anti-reflection coatings for ZnO/Si heterojunction solar cells," Ceramics International, **49**(23), Part A, 37118-37126 (2023). <https://doi.org/10.1016/j.ceramint.2023.08.313>
- [10] A. Roy, and M. Benhaliliba, "Investigation of ZnO/p-Si heterojunction solar cell: Showcasing experimental and simulation study," Optik, **274**, 170557 (2023). <https://doi.org/10.1016/j.ijleo.2023.170557>
- [11] M.-R. Zamani-Meymian, N. Naderi, and M. Zarehshahi, "Improved n-ZnO nanorods/p-Si heterojunction solar cells with graphene incorporation," Ceramics International, **48**(23), Part A, 34948-34956 (2022). <https://doi.org/10.1016/j.ceramint.2022.08.084>
- [12] D. Das, and L. Karmakar, "Optimization of Si doping in ZnO thin films and fabrication of n-ZnO:Si/p-Si heterojunction solar cells," Journal of Alloys and Compounds, **824**, 153902 (2020). <https://doi.org/10.1016/j.jallcom.2020.153902>
- [13] S. Maity, and P.P. Sahu, "Efficient Si-ZnO-ZnMgO heterojunction solar cell with alignment of grown hexagonal nanopillar," Thin Solid Films, **674**, 107-111 (2019). <https://doi.org/10.1016/j.tsf.2019.02.007>
- [14] Q. Yu, H. Zhao, and Y. Zhao, "The study of optical-electrical properties of ZnO(AZO)/Si heterojunction," Current Applied Physics, **57**, 111-118 (2024). <https://doi.org/10.1016/j.cap.2023.11.008>
- [15] M. Manoua, et al., "Optimization of ZnO thickness for high efficiency of n-ZnO/p-Si heterojunction solar cells by 2D numerical simulation," in: 2020 IEEE 6th International Conference on Optimization and Applications (ICOA), (Beni Mellal, Morocco, 2020), pp. 1-5, <https://doi.org/10.1109/ICOA49421.2020.9094491>
- [16] L. Chabane, N. Zebbar, M. Trari, and M. Kechouane, "Opto-capacitive study of n-ZnO/p-Si heterojunctions elaborated by reactive sputtering method: Solar cell applications," Thin Solid Films, **636**, 419-424 (2017). <https://doi.org/10.1016/j.tsf.2017.06.041>
- [17] Y. Murat, and A. Kocyigit, "Characterization of Al/In: ZnO/p-Si photodiodes for various In doped level to ZnO interfacial layers," Journal of Alloys and Compounds, **768**, 1064-1075 (2018).
- [18] K. Mosalagae, D.M. Murape, and L.M. Lepodise, "Effects of growth conditions on properties of CBD synthesized ZnO nanorods grown on ultrasonic spray pyrolysis deposited ZnO seed layers," Heliyon, **6**(7), e04458 (2020). <https://doi.org/10.1016/j.heliyon.2020.e04458>
- [19] J. Wang, J. Wang, J. Ding, Y. Wei, and J. Zhang, "Preparation of ZnO compact layer using vacuum ultraviolet for dye-sensitized solar cells," Solid State Sciences, **127**, 106860 (2022). <https://doi.org/10.1016/j.solidstatesciences.2022.106860>
- [20] C.E. Pachón, L.F. Mulcué-Nieto, and E. Restrepo, "Effect of band alignment on the n-InAlN/p-Si heterojunction for solar cells: a numerical study," Materials Today Energy, **17**, 100457 (2020). <https://doi.org/10.1016/j.mtener.2020.100457>
- [21] N.A. Mahammedi, H. Gueffaf, B. Lagoun, and M. Ferhat, "Numerical simulation and optimization of a silicon clathrate-based solar cell n-Si136/p-Si2 using SCAPS-1D program," Optical Materials, **107**, 110043 (2020). <https://doi.org/10.1016/j.optmat.2020.110043>

## ПОКРАЩЕННЯ СОНЯЧНИХ ЕЛЕМЕНТІВ НА ОСНОВІ ZnO/Si ГЕТЕРОПЕРЕХОДІВ: КОМБІНОВАНИЙ ЕКСПЕРИМЕНТАЛЬНИЙ ТА СИМУЛЯЦІЙНИЙ ПІДХІД

Фахріддін Т. Юсупов, Тохірбек І. Рахмонов, Мехріддін Ф. Ахмаджонов,  
Мумінджон М. Мадрахімов, Шерзод Ш. Абдуллаєв

Ферганський політехнічний інститут, Фергана, Узбекистан

У цьому дослідженні ми розглядаємо виготовлення та оптимізацію сонячних елементів на основі ZnO/Si гетеропереходів для підвищення їхньої ефективності шляхом точного контролю властивостей електронної спорідненості та ширини забороненої зони. Тонкі плівки ZnO синтезували методом термічного окислення у високовакуумній камері з подальшим відпалом для покращення кристалічності та електричних характеристик. Фотовольтаїчна продуктивність сонячних елементів на основі ZnO/Si гетеропереходів систематично характеризувалася, а симуляції за допомогою Quantum ESPRESSO використовувалися для вдосконалення електронних властивостей ZnO. Наші результати показують значні покращення напруги холостого ходу, густини струму короткого замикання та загальної ефективності перетворення. Оптимізація сонячних елементів на основі ZnO/Si гетеропереходів включає покращення електронних властивостей тонких плівок ZnO. Симуляції за допомогою Quantum ESPRESSO використовувалися для оптимізації структури ZnO, обчислення зонної структури та густини станів (DOS), а також дослідження впливу легування Ga та Mg на електронні властивості ZnO. Першим кроком у нашому дослідженні була структурна оптимізація ZnO для визначення його найнижчої енергетичної конфігурації. Оптимізація інженерії зсуву зони для покращення ефективності фотовольтаїчних елементів n-ZnO/p-Si виявилася критично важливою. Легування ZnO Ga та Mg покращило узгодження зон з Si, зменшило втрати рекомбінації та підвищило рухливість носіїв заряду. Наші висновки підкреслюють потенціал оптимізованих сонячних елементів на основі ZnO/Si гетеропереходів для високоефективного перетворення сонячної енергії, демонструючи їхню життєздатність як економічно вигідні та ефективні рішення для відновлюваних джерел енергії. Це дослідження підкреслює важливість точної інженерії матеріалів та симуляційної оптимізації у розробці вдосконалених фотовольтаїчних пристроїв.

**Ключові слова:** оксид цинку (ZnO); термічне окислення; гетероперехідні діоди; оптоелектронні програми; нанокристалічна структура; оптична заборонена зона; електричні властивості; вольт-амперні (ВАХ) характеристики; температура основи; спектри фотолюмінесценції